IC/IR/2005/017
INTERNAL REPORT
(Limited Distribution)

United Nations Educational Scientific and Cultural Organization
and
International Atomic Energy Agency

THE ABDUS SALAM INTERNATIONAL CENTRE FOR THEORETICAL PHYSICS

A THERMAL-OPTICAL ANALYSIS COMPARISON BETWEEN SYMMETRIC TUBULAR ABSORBER COMPOUND PARABOLIC CONCENTRATING SOLAR COLLECTOR WITH AND WITHOUT ENVELOPE

Réné Tchinda[1]
Fotso Victor University Institute of Technology, University of Dschang,
P.O. Box 134, Bandjoun, Cameroon
and
The Abdus Salam International Centre for Theoretical Physics, Trieste, Italy.

Abstract

Equations describing the heat transfer in symmetric, compound parabolic concentrating solar collectors (CPCs) with and without envelope have been established. The model takes into account the non linear behavior of these two systems. A theoretical numerical model has been developed to outline the effect of the envelope on the thermal and optical performance of CPCs. The effects of the flow rate, the plate length, the selective coating, etc. are studied. The over-all thermal loss coefficient and the enclosure absorption factor for both types are defined. It is found that the efficient configuration has an envelope. Theoretical computed values are in good agreement with the experimental values published in the literature.

MIRAMARE – TRIESTE
November 2005

[1] Regular Associate of ICTP.

Nomenclature

A: area (m^2)
C: specific heat (J/Kg °K)
C_p: specific heat at constant pressure (J/ Kg °K)
C_R: Concentration ratio
h : heat transfer coefficient (W/m^2 °K)
F': collector efficiency factor
F_A: enclosure absorption factor
F_R: collector heat removal factor
I : solar intensity (W/m^2)
L: length of the tube (m)
M: mass (Kg)
$\dot{m}$: mass flow (Kg/s)
<n>: number of reflection
P: gap optical loss factor
P_r: Prandtl number
q_u: heat flow (W/m^2)
r: radius (m)
R_a: Raleigh number
R_e: Reynold number
T: temperature (°K)

$$T_{fm} = \frac{1}{L}\int_0^L T_f(x,t)\,dx \qquad (°K)$$

$\Delta T=T_b-T_s$
U_L: overall heat loss coefficient ($W/m^2°K$)

Greek letters

α: absorptance
ρ: reflectance
τ:transmittance
σ: Stefan Boltzman constant ($W/m^2°K^4$)
μ: dynamic viscosity (Kg/ms)
ε: emittance
η: thermal efficiency

Subscripts

b: ambient
c : collector cover
e: receiver envelope, inlet
o: Outlet
r: receiver
ri: inside radius
ro: outside radius
R: radiative
s: sky
m: mirror
f: fluid
0: optical efficiency

1- Introduction

In any solar energy application it would be desirable to theoretically analyze as extensively as possible any given system before embarking on the construction of any one for installation. The cost-effective designs can be based partly on optimization studies. In some appliances, such as compound parabolic concentrators (CPC), an analysis can be carried out with less difficulty. It is possible to identify the parameters that control the performance of the system. Based on theoretical analyses, a suitable system for particular appliances can be designed.

There have been a number of reports of the CPC's optical and thermal characteristics with respect to concentration, acceptance angle, operating temperatures, etc. In most cases, the analyses are based on intuition [1] or are over simplified [2]. An attempt was made by Prapas et al. [3] to detail the heat exchanges encountered in CPCs and to predict the effects of parametric changes on the collector's performance. But Hsieh [2] and Prapas et al. [3] assume that reflector, absorber and cover plate are at constant temperatures. This assumption is not realistic. Eames and Norton [4,5] have produced a correlation for the variation of internal convective heat transfer in low-concentration ratio CPCs. Using these correlations and the model of heat exchanges proposed by Prapas et al [3], Kothdiwala et al. [6] have investigated the effect of the CPC inclination, the latitude and tracking configuration of the CPC system on the performance. Tchinda et al. [7] developed an analysis of thermal transfer taking into account the axial heat transfer from one end to another in a CPC collector, the nonuniform temperature of the absorber, the envelope and the aperture cover, and the geometric characteristics constant. The model of the CPCs studied by those authors is one with the receiver enclosed within a concentric transparent envelope with the intermediate annulus. Recently Kothdiwala et al. [8] have proposed for the convective heat transfer in CPCs, a correlation between the Nusselt and the Grashof numbers. They have considered CPC designs that range from a tubular absorber with envelope to one without envelope.

However, a close examination of the papers mentioned above reveals that in most of them the efficiency was calculated using efficiency equations developed according to the Hottel-Willier-Wortz-Bliss formalism [9]. Eames and Norton [9] presented the limitation of this formalism and proposed a new approach. In this approach, a procedure for analyzing collector performance data is derived which takes into account non linear behavior. The major advantage of this new procedure, over those employed previously, is that different solar collector performance characteristics can now be readily normalized to a common set of environment conditions. But, in this approach, the fluid outlet temperature

T_{fo} and the receiver temperature T_r used by Eames and Norton [9] are given by two relations which cannot take into account the fraction of the beam radiation absorbed by the cover, the envelope (type 1) and the receiver jacket. Fraidenraich et al. [10] proposed a mathematical model for the optical and thermal performance of the CPC with temperature-dependent heat loss coefficient. An attempt has been made by Oommen and Jayaraman [11] to design and fabricate a V groove CPC with reduced gap losses. Recent work in the area of CPC systems include the design, construction and test results of the low concentrator CPC type collector with convection controlled by honeycomb TIM material by Colleras-Pareira and Carvalho [12] and of the truncated CPC with a flat absorber under non-steady conditions by Pramuang and Exell [13].

This paper seeks to quantify the heat transfer within compound parabolic concentrating solar energy collectors with and without envelope. The procedure used takes into account the non linear behavior of the two systems. The thermal performances of the two designs of the same dimensions under identical conditions of insulation, inlet temperature and mass flow rate, are compared. Then, the effect of some of the design parameters such as the CPC length, the flow rate, the selective coating, etc. are discussed. In addition, the results obtained from the models are compared with those obtained from the experimental.

2- Structure of CPC and Mathematical modeling

In this work we plan to discuss two configurations of the compound parabolic concentrating solar collector shown in figure 1(a and b). They differ from each other in the presence of a receiver envelope. In Type 1, there is a receiver envelope; weather Type 2 is a CPC without a receiver envelope.

In order to simplify the analysis, the following main assumptions are made:

1- The reflector surface is free from imperfections and fabrication errors, and the entire CPC including the focal receiver is aligned accurately.

2- The reflection of radiation from the parabolic reflector is being taken into account by the apparent reflectance $\rho_m^{\langle n \rangle}$. In this analysis <n> is considered as a constant.

3- The direction of the solar radiation incident on various components in the collector can be found through geometry. Any reflection from these components, particularly multireflections from the parabolic reflector, will cause a reorientation of the rays to the effect that the rays' reflection pattern becomes exceedingly difficult to follow without reliance on a detailed ray tracing. To facilitate the analysis, these reflections are treated as

diffuse and their energy accounted for in terms of diffuse reflectivities [2]. The succeeding absorption and transmission processes inside the CPC are also diffuse and are accounted for in terms of diffuse properties.

4- The physical and the material optical properties are assumed to be independent of temperature. The aperture, the envelope and the receiver have uniform temperature distributions.

The equations that govern the behavior of the system are obtained by considering the energy balance at each component of the system separately. For the Type 1 CPC collector, the following equations are obtained for an infinitesimal element and in both equations (1) and (3) k=e.

For the transparent cover

$$M_c C_{pc} \frac{\partial T_{cj}}{\partial t} = q_{cj}(t) + h_{k/cj}(T_k - T_{cj}) + h_{Rk/cj}(T_k - T_{cj}) - h_{cj/b}(T_{cj} - T_b) - h_{Rcj/s}(T_{cj} - T_s) \quad (1)$$

with t>0.

For the envelope

$$M_e C_{pe} \frac{\partial T_e}{\partial t} = q_e(t) + h_{Rr1/e}(T_{r1} - T_e) - h_{e/c1}(T_e - T_{c1}) - h_{Re/c1}(T_e - T_{c1}) + h_{r1/e}(T_{r1} - T_e) \quad (2)$$

with t>0.

For the receiver

$$M_r C_{pr} \frac{\partial T_{rj}}{\partial t} = q_{rj}(t) - h_{Rrj/k}(T_{rj} - T_k) - q_{uj} - h_{rj/k}(T_{rj} - T_k) \quad (3)$$

For the fluid flow

$$\rho_f \pi r_{ri}^2 C_{pf} \frac{\partial T_{fj}}{\partial t} = -C_{pf} \dot{m} \frac{\partial T_{fj}}{\partial x} + 2\pi r_{ri} q_{uj} \quad (4)$$

with t>0 and 0<x<L.

There are only three equations for the Type 2 CPC collector. Equation (2) is not applicable. In equation (1), k=r_2 and in equation (3), k=c_2.

In both equations $q_{cj}(t)$, $q_e(t)$ and $q_{rj}(t)$ are respectively the absorbed solar radiation incident on the cover, the solar radiation absorbed by the receiver envelope (Type 1) and the beam radiation absorbed by the receiver jacket. The expressions of these quantities are recalled in the appendix. The instantaneous useful thermal power delivery q_{uj} (see equations (3) and (4)) of the collector depends on the position along the absorber x, on absorber temperature T_{rj} and on fluid temperature (T_{fj}):

$$q_{uj} = U_f (T_{rj} - T_{fj}) \quad (5)$$

Since the absorptance of the cover and the thermal capacities of the components of the collector are small, we neglect them. However, the functioning of the collector remains variable with time because it depends on the unsteady solar intensity. Eliminating T_{cj}, T_e and T_{rj} from the simplified equations obtained, one gets:

$$C_{pf}\,\dot{m}\,\frac{dT_{fj}}{dx} = 2\pi r_{ri}\left[S_{pj} - U_{Lj}\left(T_{fj} - T_b\right)\right]F'_j \tag{6}$$

where j=1 for the Type 1 CPC collector and

$$S_{p1} = q_{r1}(t) + \frac{(h_{Re/c1} + h_{e/c1} + h_{c/b} + h_{Rc1/s})U_{L1}}{(h_{Re/c1} + h_{e/c1})(h_{c1/b} + h_{Rc1/s})}q_e(t) + \frac{U_{L1}q_{c1}(t)}{h_{c1/b} + h_{Rc1/s}} - \frac{\Delta Th_{Rc1/s}U_{L1}}{h_{c1/b} + h_{Rc1/s}} \tag{7}$$

$$U_{L1} = \frac{(h_{Rr1/e} + h_{r1/e})(h_{Re/c1} + h_{e/c1})(h_{c1/b} + h_{Rc1/s})}{(h_{Rr1/e} + h_{r1/e} + h_{Re/c1} + h_{e/c1})(h_{Re/c1} + h_{e/c1} + h_{c1/b} + h_{Rc1/s}) - (h_{Re/c1} + h_{e/c1})^2} \tag{8}$$

$$F'_1 = \frac{1}{U_{L1}}\left[\frac{1}{U_f} + \frac{1}{U_{L1}}\right]^{-1} \tag{9}$$

j=2 for the Type 2 CPC collector and

$$S_{p2} = q_{r2}(t) + \frac{(h_{r2/c2} + h_{Rr2/c2})q_{c2}(t) - \Delta Th_{Rc2/s}(h_{r2/c2} + h_{Rr2/c2})}{h_{r2/c2} + h_{Rr/c2} + h_{c2/b} + h_{Rc2/s}} \tag{10}$$

$$U_{L2} = \frac{(h_{r/c2} + h_{Rr/c2})(h_{c2/a} + h_{Rc2/s})}{h_{r/c2} + h_{Rr/c2} + h_{c2/a} + h_{Rc2/s}} \tag{11}$$

$$F'_2 = \frac{U_f(h_{r2/c2} + h_{Rr2/c2} + h_{c2/b} + h_{Rc2/s})}{(U_f + h_{r2/c2} + h_{Rr2/c2})(h_{r2/c2} + h_{Rr2/c2} + h_{c2/b} + h_{Rc2/s}) - (h_{r2/c2} + h_{Rr2/c2})^2} \tag{12}$$

If we assume that F'_j and U_{Lj} are temperatures independent in position, the solution for the temperature at any position x (subject to the condition that the inlet fluid temperature is T_{fe}) is given by:

$$\frac{T_{fj} - T_b - (S_{pj}/U_{Lj})}{T_{fe} - T_b - (S_{pj}/U_{Lj})} = \exp\left[-\frac{2\pi r_{ri}U_{Lj}F'_j}{C_{pf}\dot{m}}x\right] \tag{13}$$

If the collector has the length L in the direction of the flow, the outlet fluid is found by substituting L by x in equation (13), so one obtains:

$$\frac{T_{foj} - T_b - (S_{pj}/U_{Lj})}{T_{fe} - T_b - (S_{pj}/U_{Lj})} = \exp\left[-\frac{A_r U_{Lj}F'_j}{C_{pf}\dot{m}}\right] \tag{14}$$

The useful thermal power extracted from the system in the form of heat by the fluid is calculated from the relationship:

$$Q_{uj} = \dot{m}\,C_f(T_{foj} - T_{fe}) \tag{15}$$

where $(\dot{m}C_f)$ refers to the thermal capacitance rate for the circulating fluid. The efficiency is found to be:

$$\eta_{instj} = \frac{Q_{uj}}{A_C I(t)} \tag{16}$$

Using equations (14) and (15), η_{instj} becomes:

$$\eta_{instj} = \left(\eta_{0j} + F_{Aj}\right) F_{Rj} - \frac{U_{Lj}}{C_R I(t)} F_{Rj} \left(T_{fe} - T_b\right) \tag{17}$$

where the optical efficiency is given :

for the Type 1 CPC collector, j=1

$$\eta_{01} = \overline{\tau}_c \rho_m^{\langle n \rangle} \overline{\tau}_e P \ \overline{\alpha}_r \left(1 + \overline{\rho}_e \rho_r \frac{A_r}{A_e}\right) \tag{18}$$

and for the Type 2 CPC collector j=2

$$\eta_{02} = \overline{\tau}_c \rho_m^{\langle n \rangle} P \ \overline{\alpha}_r \left(1 + \overline{\rho}_r \overline{\rho}_c \frac{A_r}{A_c}\right) \tag{19}$$

Equations (18) and (19) are related to the process in which the beam or direct component of the incident solar radiation is transmitted through the component of the CPC and absorbed by the receiver. Table 1 shows an examination of equations (18) and (19) when C_R tends to infinity and when C_R = 1 (conditions corresponding to the concentration ratio of a flat plate collector [2]). The results show that, η_{0j} reaches its maximum value when C_R=1 and approaches the minimum value at the limit when C_R tends to infinity. Comparing equations (18) and (19), the ratio gives:

$$\frac{\eta_{02}}{\eta_{01}} = \frac{1 + \rho_c \rho_r \frac{A_r}{A_c}}{\tau_e \left(1 + \rho_e \rho_r \frac{A_r}{A_e}\right)} \succ 1 \tag{20}$$

This result shows that the presence of the envelope contributes to create optical losses. In the literature, optical efficiency is given by:

$$\eta_{01} = \frac{\overline{\tau}_c \rho_m^{\langle n \rangle} \overline{\tau}_e P \ \overline{\alpha}_r}{1 - \overline{\rho}_e \rho_r \frac{A_r}{A_e}} \tag{21-a}$$

for Type 1 [2,5,11], and

$$\eta_{02} = \overline{\tau}_c \rho_m^{\langle n \rangle} \overline{\alpha}_r \tag{21-b}$$

for Type 2 [28].

The optical efficiency determined from equations (18) and (19) with the optical properties of the materials listed in this paper has the values 59% for Type 1 and 66% for Type 2. The value of the gap size used is G_p=0.8 cm, which corresponds to the operating temperature under consideration [28]. This condition can easily be met without excessive optical losses in the gap, because tube radius of the order of 0.025 m is practical for such a collector, and the resulting optical loss is of the order of 6% [28]. The optical efficiency found by the relations (18) and (19) agree with the optical efficiency found by the relations (21-a and b) with an average error of 5% for Type 2.

In equation (17), F_{Aj} is named the enclosure absorption factor [2,7]. It is given by the relationship:

for the Type 1 CPC collector

$$F_{A1} = \frac{\left(h_{Re/c1} + h_{Rc1/s} + h_{c1/b} + h_{e/c1}\right) U_{L1} \overline{\tau}_c \rho_m^{\langle n \rangle} \overline{\alpha}_e}{\left(h_{e/c1} + h_{e/c1}\right)\left(h_{c1/b} + h_{Rc1/s}\right)} \left\{1 + \overline{\rho}_c \overline{\rho}_e \rho_m^{2\langle n \rangle} \frac{A_e}{A_c} + \overline{\rho}_r \overline{\tau}_e\right\} + \frac{\left(\overline{\alpha}_c + \overline{\alpha}_c \overline{\tau}_c \overline{\rho}_e \rho_m^{2\langle n \rangle}\right) U_{L1}}{h_{c/b} + h_{Rc1/s}} - \frac{\Delta T \; h_{Rc1/s} U_{L1}}{C_R \left(h_{c1/b} + h_{Rc1/s}\right) I(t)} \quad (22)$$

and for the Type 2 CPC collector

$$F_{A2} = \frac{\left(h_{Rr/c2} + h_{r2/c2}\right)}{\left(h_{Rr2/c2} + h_{r2/c2} + h_{c2/b} + h_{Rc2/s}\right)} \left\{\overline{\alpha}_c + \overline{\alpha}_c \overline{\tau}_c \overline{\rho}_r \rho_m^{2\langle n \rangle} - \frac{\Delta T \; h_{Rc2/s}}{I(t) \; C_R}\right\} \quad (23)$$

Equation (16) introduces the heat removal factor defined as:

$$F_{Rj} = \frac{G \; C_f C_R}{U_{Lj}} \left\{1 - \exp\left(-\frac{U_{Lj} F'_j}{G \; C_f C_R}\right)\right\} \quad (24\text{-a})$$

where $G = \dot{m} / A_C$ (24-b)

The daily efficiency η_d of the CPC collector (Types 1 and 2) is calculated from the relationship:

$$\eta_{dj} = \frac{\int_{t_r}^{t_s} \dot{m} \; C_f \left(T_{foj} - T_{fe}\right) dt}{A_C \int_{t_r}^{t_s} I(t) \, dt} \quad (25)$$

where t_r and t_s are respectively the instants of sunrise and sunset.

3- Numerical Input

Meteorological data

The mean values of the ambient temperature and global radiation in May at Garoua (9°20'N;13°23'E; altitude 241 m) are used [7,14]. The sky temperature is assumed to be 6°c less than the ambient temperature [7,15].

Radiative heat-transfer coefficients

In most of the calculations a constant value of the radiative heat-transfer is often used for all values of G and L. In our opinion this may not be justified as h_R depends on the temperature of the radiating surface, which in turn depends on the values of G and L [16]. In the present work, instead of using a constant value of h_R for different sets, we have calculated it for each set from an iterative method as follows.

The radiative heat loss coefficient $h_{Rcj/s}$ between the surface cover and the sky is calculated from the relationship:

$$h_{Rcj/s} = \sigma\ \varepsilon_c (T_{cj}^2 + T_s^2)(T_{cj} + T_s) \frac{A_C}{A_{ro}} \tag{26}$$

The radiative transfer coefficient $h_{Re/c1}$ between an envelope and the cover is calculated using relation [7]:

$$h_{Re/c1} = \frac{\sigma \left(T_e^2 + T_{c1}^2\right)\left(T_e + T_{c1}\right)}{\frac{1}{\varepsilon_e} + \frac{A_e}{A_c}\left(\frac{1}{\varepsilon_c} - 1\right)} \frac{A_e}{A_{r0}} \tag{27}$$

The coefficient of heat loss by radiation $h_{Rrj/i}$ from the receiver jacket to the envelope (Type 1) or from the receiver jacket to the cover (Type 2) is given by:

$$h_{Rrj/i} = \frac{\sigma \left(T_{rj}^2 + T_i^2\right)\left(T_{rj} + T_i\right)}{\frac{1}{\varepsilon_r} + \frac{A_{r0}}{A_i}\left(\frac{1}{\varepsilon_i} - 1\right)} \tag{28}$$

Convective heat transfer coefficients

The forced convection heat transfer coefficient $h_{cj/b}$ estimated as a function of the wind speed by Duffie and Beckman [17] is defined by the relationship:

$$h_{cj/b} = (5.7 + 3.8V)\frac{A_c}{A_{r0}} \tag{29}$$

V (m/s) is the wind speed .

Mullick and Nanda, recalled by Bhowmik and Mullick [18] have examined several correlations for the coefficient of heat transfer by natural convection between horizontal concentric cylinders. Among them are the correlations of Fishenden and Saunders [19], Itoh et al [20], Raithby et al. [21] and Kuehn et al. [22]. For the present application they

have recommended the correlation due to Raithby and Hollands and modified by Bhowmik and Mullick [18]. The convective heat transfer coefficient is defined as:

$$h_{r1/e} = \frac{2\pi L K_{eff}}{(2\pi L r_{r0}) \ln\left(\frac{r_e}{r_{r0}}\right)} \tag{30}$$

$$K_{eff} = 0.3152\ K\ (R_{acc})^{0.25} \quad \text{and} \quad K = 0.000486\ T_{mre}^{0.7} \tag{31}$$

where the Raleigh number is defined as [18]:

$$R_{acc} = 0.1025\ \ 10^{20\left[\frac{T_{r1}-T_e}{T_{mre}^{4.4}}\right]} \frac{\left[\ln\left(\frac{r_e}{r_{r0}}\right)\right]^2}{\left[\frac{1}{D_{r0}^{0.6}} + \frac{1}{D_e^{0.6}}\right]^5} \overline{P}_r \tag{32}$$

$$\text{and } T_{mre} = 320 + (0.11\varepsilon_r + 0.57)(T_{r1} - 330) \tag{33}$$

The average Prandtl number is taken as 0.69 [18].

The convective part $h_{i/cj}$ can be calculated by using the formula [2,7]

$$h_{i/cj} = \left[3.25 + 0.0085\ \frac{T_i - T_{cj}}{4 r_{r0}}\right] \frac{A_\alpha}{A_{r0}} \tag{34}$$

where α=i=e for Type 1, α=cj and i=r2 for Type 2. A close examination of this relation in the two designs shows that $h_{e/c1}<h_{r2/c2}$. This result can be explained by the fact that, the lower temperature at the envelope surface gives rise to a lower rate of convective heat transfer than would be ensured in the envelope's absence.

On the basis of unit receiver jacket area, U_f can now be formulated as follows [2,7]:

$$U_f = \left[\frac{r_{r0}}{\lambda_f} \ln\left(\frac{r_{r0}}{r_{ri}}\right) + \frac{r_{ri}}{h_f r_{r0}}\right]^{-1} \tag{35}$$

where the first term of the expression inside the brackets estimates the material conductive resistance and the second the convective film resistance. The factor h_f appearing in this equation is the convective heat transfer coefficient from the receiver to the fluid. It is given as:

$$h_f = \frac{N_{uf}\ \mu_f}{d_{ri}} \tag{36}$$

The Nusselt number N_{uf} is calculated by the Sieder and Tate correlation and is given in [23,24]

$$N_{uf} = 1.86 \left[\frac{R_{ef}\ P_{rf}\ d1}{L}\right]^{1/3} \left(\frac{\mu_f}{\mu_{fs}}\right)^{0.14} \tag{37}$$

for a laminar flow with $(R_{ef}\ P_{rf}\ d_{ri}/L)^{1/3}\left(\frac{\mu_f}{\mu_{fs}}\right)^{0.14} \geq 2$

μ_{fs} being the fluid viscosity near the tube wall

and $$N_{uf} = 0.023\ R_{ef}^{0.8} P_{rf}^{1/3}\left(\frac{\mu_f}{\mu_{fs}}\right)^{0.14} \quad (38)$$

for a turbulent flow $R_{ef} > 10{,}000$

with $$R_{ef} = \frac{4\dot{m}}{\mu_f \pi d_{ri}} \quad (39\text{-a})$$

and $$P_{rf} = \frac{\mu_f C_{pf}}{\lambda_f} \quad (39\text{-b})$$

These relationships are valid for $0.7 \leq P_{rf} \leq 16{,}700$.

Other parameters

The dimensions and other properties of the various components of the two types of collectors are as follows [2,7,25]:

Collector specifications

W= 0.1128 m, r_e= 0.0264 m, r_{ri}= 0.0222 m, r_{r0}= 0.0242 m

Material properties

$\in_c=\in_e$=0.85, $\in_r$=0.05, $\tau_c=\tau_e$=0.9, $\rho_c=\rho_e$=0.05, ρ_r=0.15, ρ_m=0.85, $\alpha_c=\alpha_e$=0.05, α_r=0.85

λ_f=1.3153 W/m°k, <n>=0.6, μ_f=1.11 kg/ms, ρ_m=0.85.

The calculations are done for three values of the CPC length L, ranging from 0.5 to 1.5 m and two values of ε_p ranging from 0.1 for a selected coating surface to ε_p=0.9 for a black painted surface. Glycerol is used as heat transfer fluid. $\dot{m}$ varies from 0.0002 to 0.0012 kgs^{-1}.

Numerical procedure

In numerical calculations, an iterative procedure is adopted to bring the effect of the temperature, depending on various heat transfer coefficients. For certain temperatures, they are first calculated by using the standard expressions given earlier. The equations are solved by assuming constant heat coefficients and then determining new solutions which will be used to generate all the heat transfer coefficients again till the values converge. The convergence criteria are given by:

$$\mathrm{Sup}\left[\max_{ji}\left|T_{fji}^{k+1}-T_{fji}^{k}\right|,\left|T_{cj}^{k+1}-T_{cj}^{k}\right|,\left|T_{e}^{k+1}-T_{e}^{k}\right|,\left|T_{rj}^{k+1}-T_{rj}^{k}\right|\right] \leq \xi \quad (40)$$

A proper choice of the ξ is important to make sure that the convergence is rich. Several tests have been made, for which ξ takes the values 10^{-2}, 10^{-3} and 10^{-4}

respectively, the results and numbers of iterations were compared. The results showed that for low values of the flux (I(t)<200 W/m^2), the value $\xi=10^{-2}$ was sufficient, while for high values of the flux I(t), $\xi\sim 8\ 10^{-4}$ was sufficient. Throughout the present calculations the value of ξ was kept constant at 10^{-5}.

4- Performance

The outlet temperatures for some values of the mass flow rate are shown in figure 2. As the mass flow rate increases, for given L and T_{fe}, the contact duration decreases consequently the outlet temperatures also decrease. For a given $\dot{m}$, the rise in temperature is least. This is because the overall heat loss coefficient (figure 3) in Type 2 is larger than that in Type 1. The difference between the two coefficients increases with $\dot{m}$. The larger overall heat loss coefficient implies that more heat would be transferred to the cover, i.e. the cover temperature will be higher in Type 2 (figure 4). The rise in outlet temperature in Type 1 is justified by the presence of the envelope (figure 1-a).

T_{f0} at 12.30 pm as a function of L is plotted in figure 5-a and b. In both Type 1 and Type 2, it increases. The trend of the curves indicates that there may be a value of L beyond which T_{f0} may become constant; that value of L will depend on $\dot{m}$. In figure 6-a and b, T_{f0} is plotted at 12.30 pm, as a function of $\dot{m}$ for some values of L. The total rise in temperature or the total heat collected by the heat transfer fluid from the tube depends on the time during which the heat transfer fluid remains in contact with the tube. As L increases, the time of contact between the heat transfer fluid and the receiver increases, consequently T_{f0} also increases. For a small plate length, T_{f0} quickly becomes constant whereas for larger plate lengths it slowly approaches a constant value.

The daily efficiency as a function of L for two values of $\dot{m}$, is plotted in figure 7. In Type 2, the daily efficiency decreases with L for a given value of $\dot{m}$, but increases with $\dot{m}$ for a given L (figure 8). As the fluid passes through the channel, it gains heat and T_f increases. For a given $\dot{m}$, the effect of L on the daily efficiency is very small and becomes negligible when $\dot{m}$ increases in type 1 (figures 7 and 8). Nevertheless, the daily efficiency increases perceptibly with $\dot{m}$ for a commercial value of L (e.g. L=1.5 m [2,5,7], see figure 8-bis). In order to study the effect of a selective coating on the performance of the CPC, calculations are performed for a black painted surface with $\in$=0.9, and a selectively coated surface with $\in$=0.1. In figure 9, the outlet temperature for both types of surfaces is plotted. The selective coating will be more effective in those cases where the outlet temperature of the heat transfer fluid is higher. It is also noted that the selective coating contributes to

suppress the radiative loss from the receiver. The effect of a selective coating will not be much in early morning hours and in late evening hours, as the outlet temperature of the fluid for both types of surfaces practically coincides.

As is shown in figure 10, an increase of the gap size lowers the daily efficiency. This is certainly being ascribed to the presence of the P in the optical efficiency (eqs 18 and 19). It is seen that, as the gap size G_p increases from 2.2 to 20 mm for Type 1 and from 1 to 20 mm for Type 2, the daily efficiency decreases about 11.38% and 8.55% respectively. Because of the increase of G_p, other parameters remain constant, the optical loss correction inside the gap (see appendix) decreases, consequently the solar radiation absorbed by the receiver jacket (see appendix) and heat transfer to the working fluid will be lower. It is also noted that the minimum value of the gap size in Type 1 is r_e-r_{ro}. If G_p< r_e-r_{ro}, the reflector will be truncated (Type 1) and this creates edge losses. In this case, the model of heat transfer developed for Type 1 is not valid. However, in many solar thermal applications, a gap between the reflector and the absorber is needed to incorporate an evacuated envelope and/or to reduce conductive heat losses since a reflector sheet in direct contact with the absorber is an efficient cooling fin [11,26].

5- Validation of the Mathematical model

In order to validate the computer modeling used in the prediction given in this paper, the computer predicted data were also compared with experiments (see figure 11) [27,28,29]. The test data were taken from a collector in conditions sufficiently close to those ones given by Hsieh [2] and Rabl et al. [28,29]. As shown in the figure 11, the agreement between the prediction and experiment appears to be satisfactory with average errors of 7.00% and 6.00% respectively for Types 1 and 2.

6- Conclusions remarks

In this work we have discussed two different types of CPCs with a view to study the effects of some of the parameters on their performances. The following conclusions are obtained:

- For a given L, the efficiency increases as G increases. A short length is more efficient than a long one.
- The selective coating changes the performance considerably.
- The most efficient configuration is Type 1.
- The effect of the gap size is somewhat smaller because of the dependency of η_0 on P.

Acknowledgments

The first author would like to thank the Associateship Scheme of the Abdus Salam International Centre for Theoretical Physics, Trieste, Italy. He also acknowledges financial support from the Swedish International Development Cooperation Agency.

Appendix

$q_{cj}(t)$, $q_e(t)$ and $q_{rj}(t)$ are been expressed according to Hsieh [2], Chakraverty et al. [25] and Tchinda et al. [7] as:

$$q_{cj}(t) = I(t)\left[\overline{\alpha}_{cj} + \overline{\alpha}_{cj}\,\overline{\tau}_{cj}\,\overline{\rho}_i\,\rho_m^{2\langle n\rangle}\right]\frac{A_c}{A_{r0}} \tag{A1}$$

$$q_e(t) = I(t)\,\overline{\tau}_{c1}\,\rho_m^{\langle n\rangle}\left[\overline{\alpha}_e + \overline{\alpha}_e\,\overline{\rho}_{c1}\,\overline{\rho}_e\,\rho_m^{2\langle n\rangle}\frac{A_e}{A_c} + \overline{\alpha}_e\,\overline{\rho}_r\,\overline{\tau}_e\right]\frac{A_c}{A_{r0}} \tag{A2}$$

$$q_{rj}(t) = I(t)\,\overline{\tau}_{cj}\,\rho_m^{\langle n\rangle}\,\overline{\tau}_i\,P\left[\overline{\alpha}_r + \overline{\alpha}_{rj}\,\overline{\rho}_{rj}\,\overline{\rho}_i\frac{A_{r0}}{A_i}\right]\frac{A_c}{A_{r0}} \tag{A3}$$

where $A_c=2WL$, $A_e=2\pi r_e L$, $A_{r0}=2\pi r_{r0}L$.

It is assumed that the diffuse mirror, envelope and receiver properties are the same as the direct properties [2,7,25]. In this case: $\overline{\tau}=\tau$, $\overline{\alpha}=\alpha$ and $\overline{\rho}=\rho$.

P's introduced in equation (A3) to correct the losses inside the gap is given by [2,7,25]:

$$P = 1 - \frac{G_p}{2\pi r_{ro}} \tag{A4}$$

References

1- Rabl A., Comparison of solar concentrators. Solar Energy 17, 255-258 (1976)
2- Hsieh C.K., Thermal analysis of CPC collectors, Solar Energy 27,19 (1981)
3- Prapas D.E., Norton B. and Probert S.D. Thermal design of compound parabolic concentrating solar energy collectors J. Solar Energy Engng 109, 161-168 (1987)
4- Eames P.C. and Norton B., Detailed parametric analyses of heat transfer in CPC solar Energy collectors. Solar Energy Vol. 50, N°4, pp. 321-338, (1993).
5- Eames P.C. and Norton B., Validated, Unified model for optics and heat transfer in line-axis concentrating solar energy collectors. Solar Energy Vol. 50, N°4, pp. 339-355, (1993).
6- Farouk Kothdiwala A., Eames P.C. and Norton B., The effect of variation of angle of inclination on the performance of low-concentration-ratio compound parabolic concentrating solar collectors., Solar Energy, vol. 55, N°4, pp. 301-309, (1995).
7- Tchinda R., Kaptouom E. and Njomo D., Study of the CPC collector thermal behaviour, Energy Convers. Mgmt Vol. 39, N° 13, 1395-1406 (1998)
8- Kothdiwala A.F., Eames P.C. and Norton B., Convective heat transfer correlations for an enclosed horizontal compound parabolic cavity solar thermal collector. Int. J. of Solar Energy, Vol. 20, pp 161-175 (2000)
9- Eames P.C. and Norton B., A non linear steady-state characteristic performance curve for medium temperature solar energy collectors, journal of solar Energy Engineering, August 1991, Vol. 113, pp. 164-171
10- Fraidenraich N., DE R. F. DE Lima, Tiba C. and Barbosa E.M., Simulation model of CPC collector with temperature dependent heat loss coefficient, Solar Energy,Vol. 65, No 2, pp. 99-110, (1999)
11- Oommen R. and Jayaraman S., Development and performance analysis of compound parabolic solar concentrators with reduced gap losses-'V' groove reflector, Renewable Energy 27, pp. 259-275,(2002)
12- Collares Pereiras M. and Carvalho M.J., New low concentration CPC type collector with convection controlled by a honeycomb TIM material: a compromise with stagnation temperature control and survival of cheap fabrication materials, ISES Solar World Congress, Solar Energy for sustainable Future, 2003
13- Pramuang S. and Exell R.H.B., Transient test of a solar air heater with a compound parabolic concentrator, Renewable Energy 30, pp. 715-728, (2005).
14- Njomo D., Modelling the heat exchanges in a solar air heater with a cover partially transparent to infrared radiation, Energy Convers. Mgmt. 31, 5 (1991).
15- Whillier A., Design factors influencing solar collectors in low temperature Engineering applications for solar energy ASHRAE, New York (1967)
16- Ashok Kumar Bhargava, Garg H.P. and Sharma V.K., Evaluation of the performance of air heaters of conventional designs, Solar Energy, vol. 29, N°6, 523-533(1982)
17- Duffie J.A. and Beckman W.A., Solar Engineering of thermal processes, 2nd edn. Wiley-Interscience, New York (1991)
18- Bhowmik N.C. and Mullick S.C., Calculation of tubular absorber heat loss factor. Solar Energy Vol. 35, N°3, 219-225 (1985)
19- Fishenden M. and Saunders O.A., An introduction to heat transfer, oxford, New York, (1950)
20- Itoh M., Fujita T., Nishiwaki N. and Hirita M., A new method of correlating heat transfer coefficients for natural convection in horizontal cylindrical annuli. Int. J. Heat Mass Transfer 13, 1364-1368 (1970)
21- Raithby G.D. and Hollands K.G.T., A general method of obtaining approximate solution to laminar and turbulent free convection problems. Advances in heat transfer 11, 265-315, Academic Press, New York, (1975).
22- Kuehn T.H. and Gldstein R.J., correlating equations for natural convection heat transfer between horizontal, circuler cylinders. Int. J. Heat Mass transfer 19 , 1127-1134, (1976)
23- Sacadura J.F., Initiation aux transferts thermiques, Tech. et Documentation 446 p., (1982)
24- Brodkey R.S. and Hershey H.C., Transport phenomena, McGaw-Hill Book company, (1988)
25- Chakraverty S, Bansal N.K. and Garg H.P., Transient analysis of a CPC collector with time dependent input function, Solar Energy 38, 3 (1987).
26- Schertz W.W., Nonimaging concentrators deliver higher temperatures for industry. Solar Engng. Mag. (1977)
27- Reed K.A., Compound parabolic concentrator collector development, Solar energy program annual report. Argonne National Laboratory, ANL - 79-16, pp 5-12 (1979)
28- Rabl A., O'Gallagher J. and Winston R., Design and test of non-evacuated solar collectors with compound parabolic concentrators, Solar Energy Vol. 25, (1980).
29- Rabl A., Goodman N.B. and Winston R., Practical design considerations for CPC solar collectors, Solar Energy 22, pp. 373-381, (1979).

Table 1: Expressions of the optical efficiency

Type of CPC	$C_R \to \infty$	$C_R=1$
1	$\overline{\tau}_c \rho_m^{\langle n \rangle} \overline{\tau}_e P \ \overline{\alpha}_r$	$\overline{\tau}_c \rho_m^{\langle n \rangle} \overline{\tau}_e P \ \overline{\alpha}_r \left(1 + \overline{\rho}_r \overline{\rho}_e \frac{A_c}{A_e}\right)$
2	$\overline{\tau}_c \rho_m^{\langle n \rangle} P \ \overline{\alpha}_r$	$\overline{\tau}_c \rho_m^{\langle n \rangle} P \ \overline{\alpha}_r \left(1 + \overline{\rho}_r \overline{\rho}_c\right)$

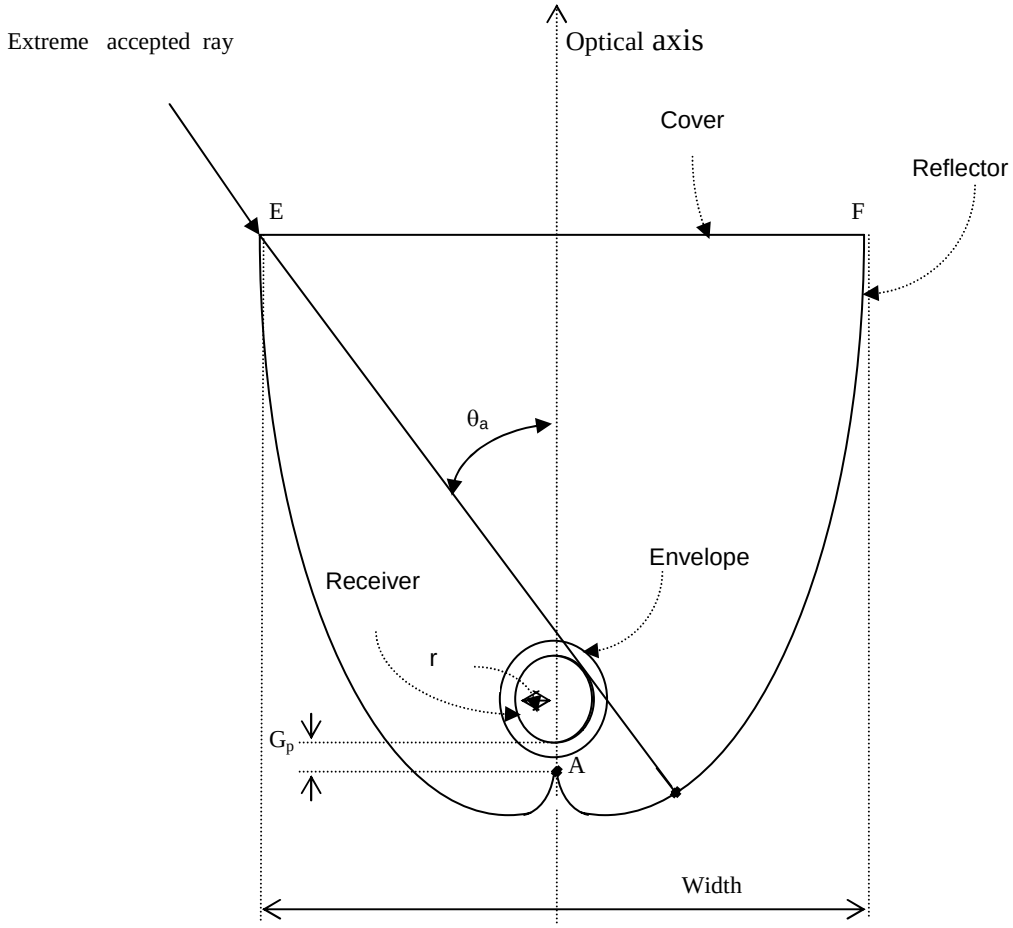

(a) Type 1)

Figure 1a: A schematic diagram showing the two types of CPC under investigation

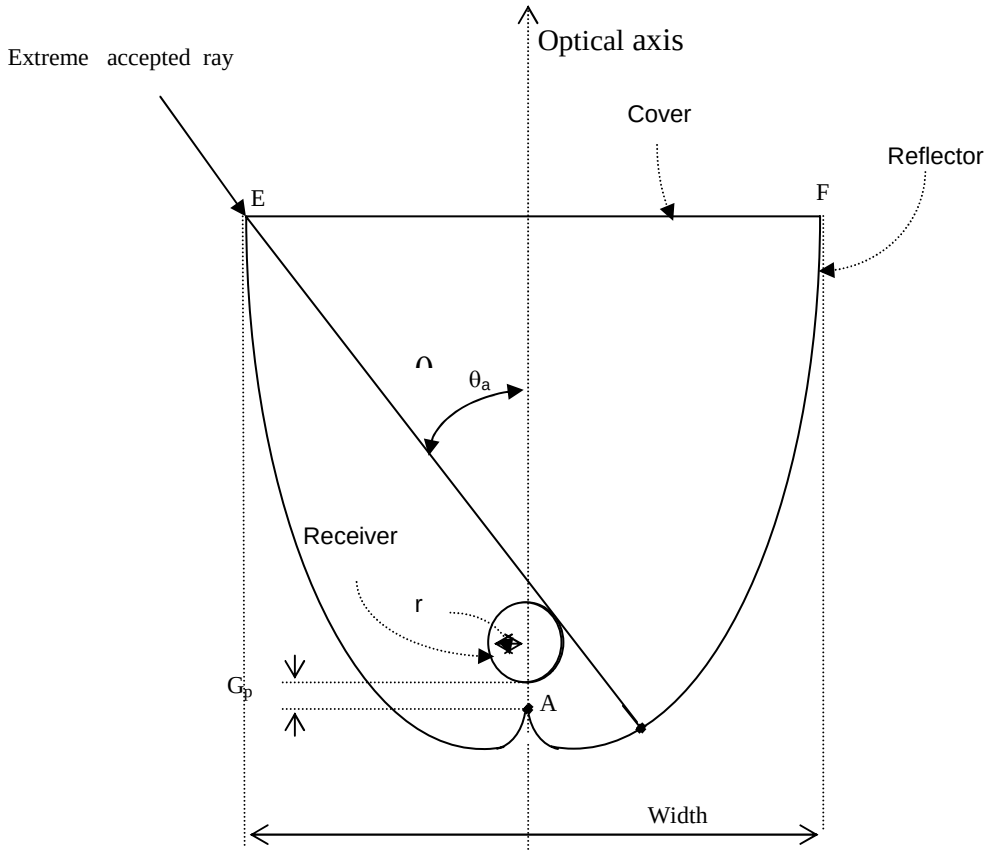

(b) Type 2)

Figure 1b: A schematic diagram showing the two types of CPC under investigation

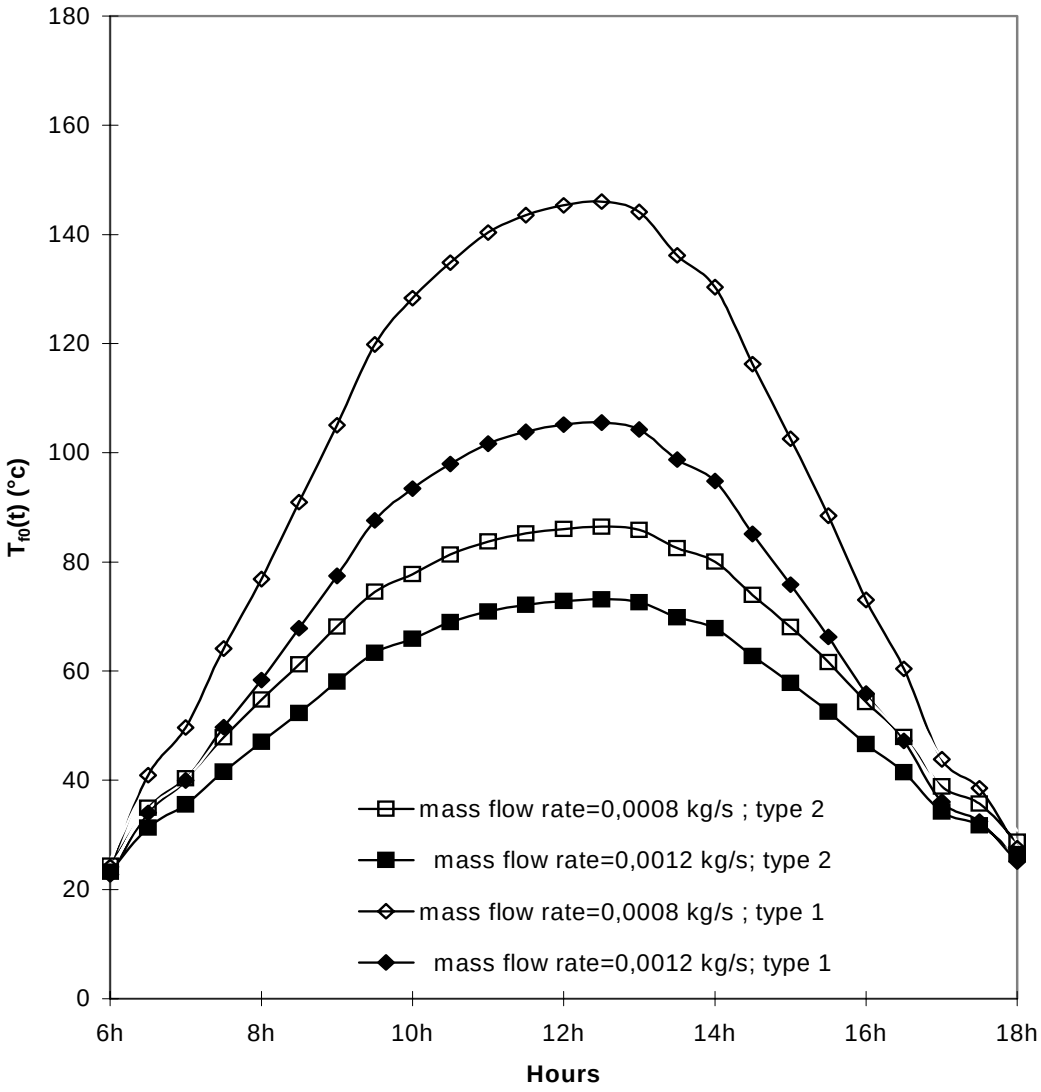

Figure 2: Effect of the glycerol mass flow rate on the hourly variations of the outlet temperature,
T_{fe}=20,0°c, V=5,0 m/s

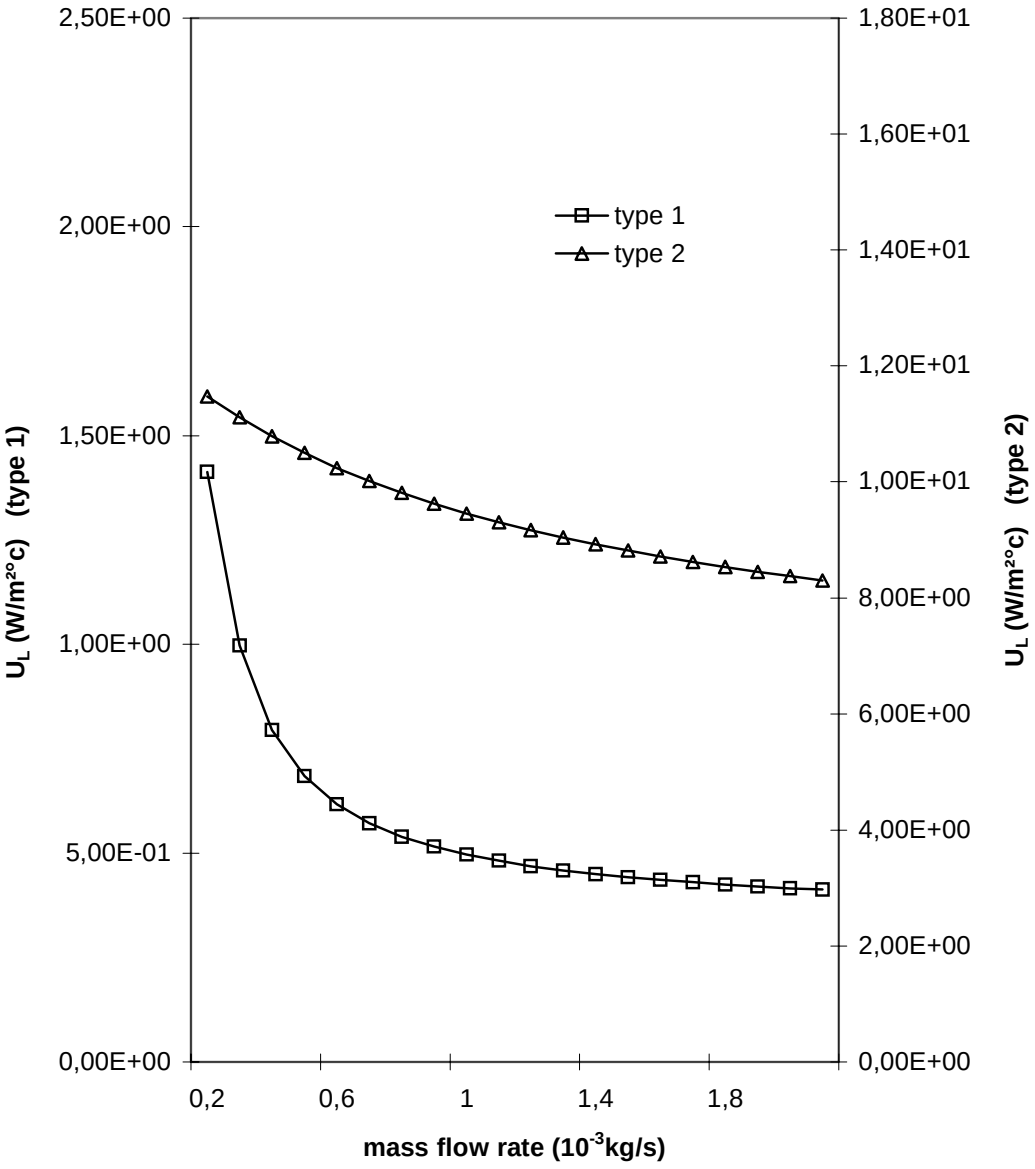

Figure 3: Effect of mass flow rate on U_L ;
T_{fe}=20,0°c, V=5,0 m/s

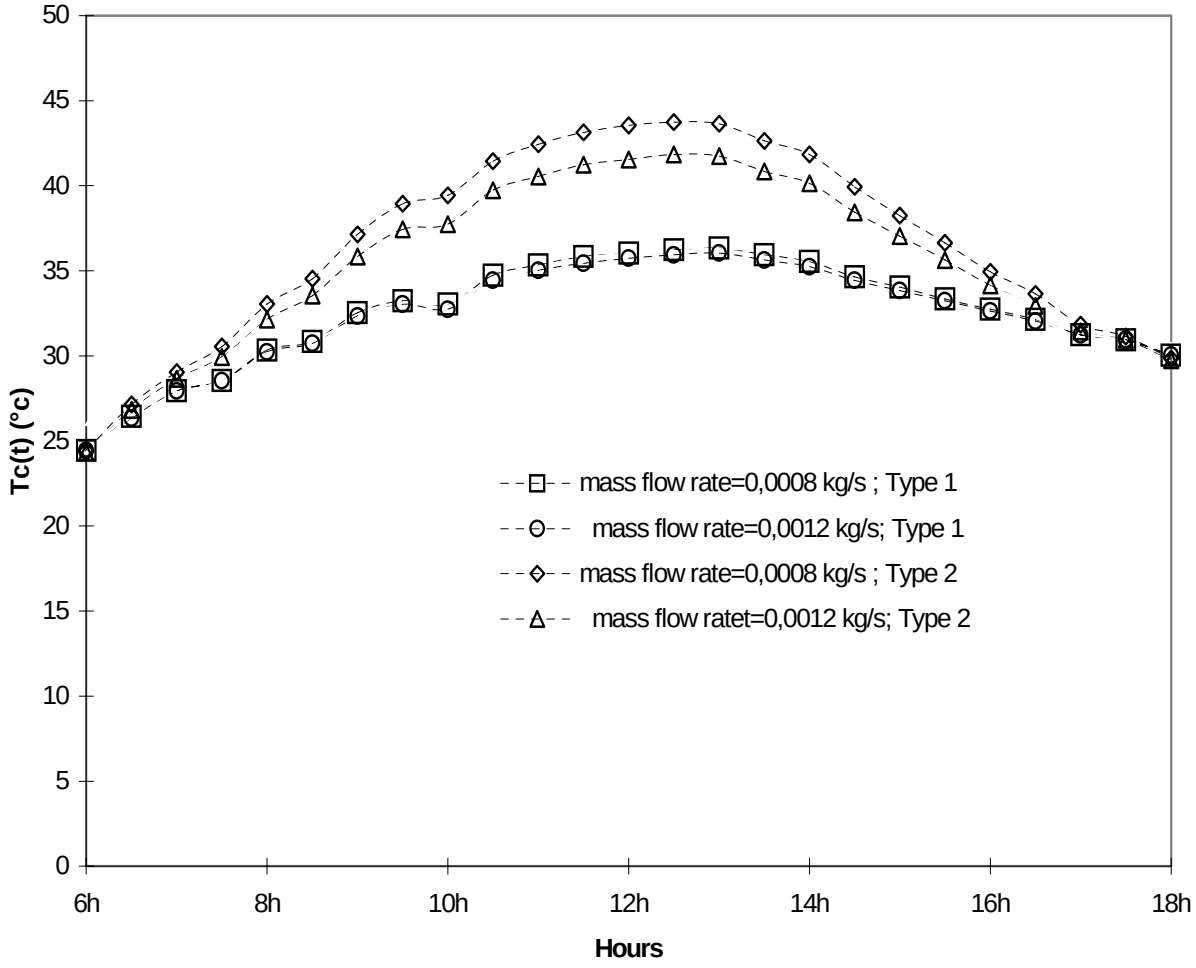

Figure 4: Variation of the temperatures of cover with hours of the day, T_{fe}=20,0°c; V=5,0 m/s

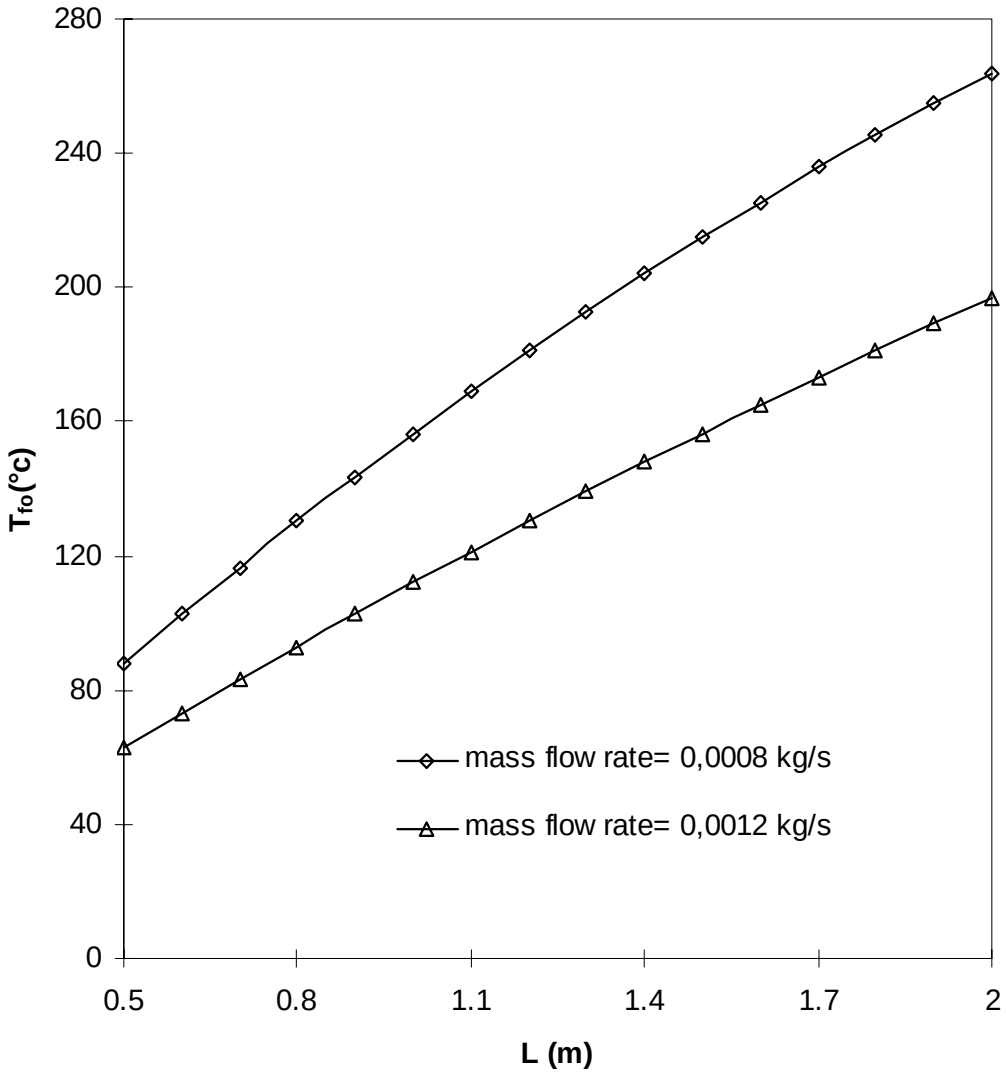

(a)

Figure 5a: The outlet temperature as function of CPC length for some values of mass flow rate. (a) Type 1, (b) Type 2

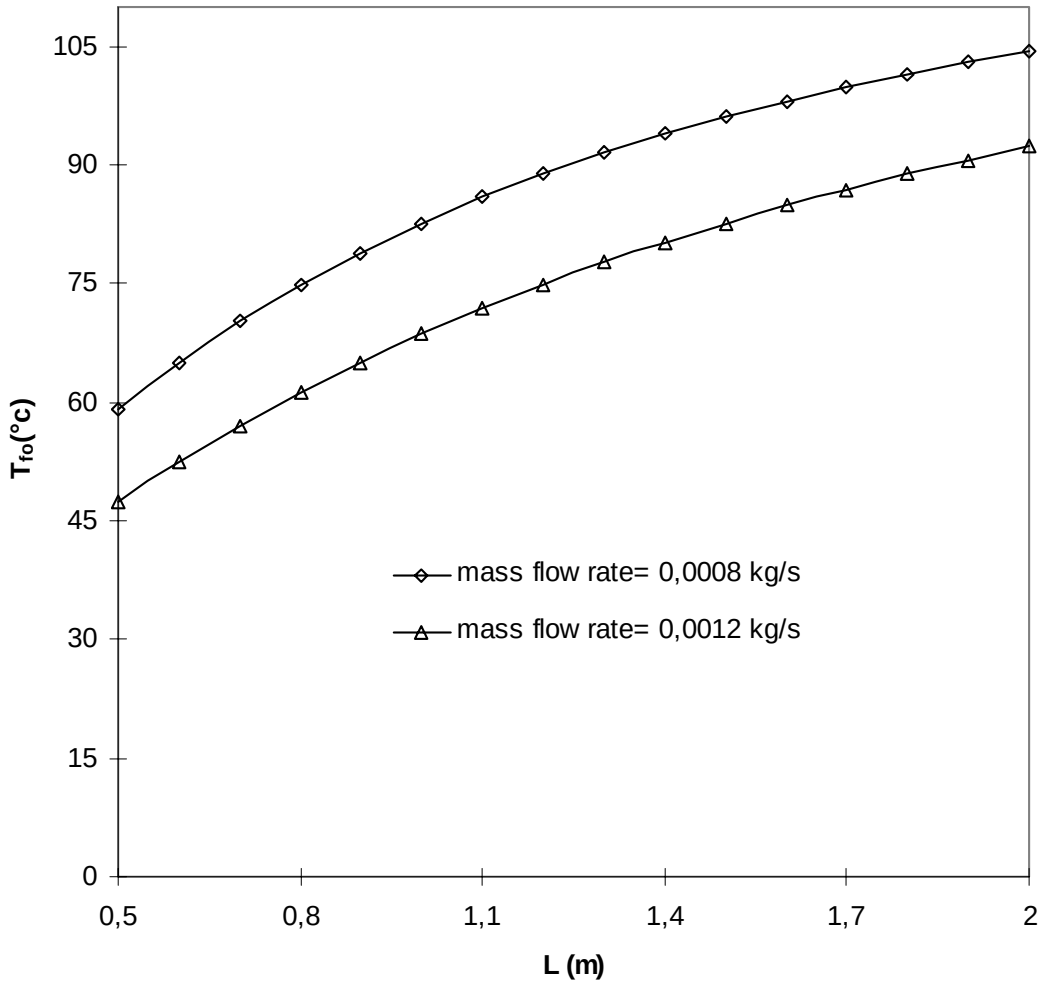

(b)

Figure 5b: The outlet temperature as function of CPC length for some values of mass flow rate. (a) Type 1, (b) Type 2

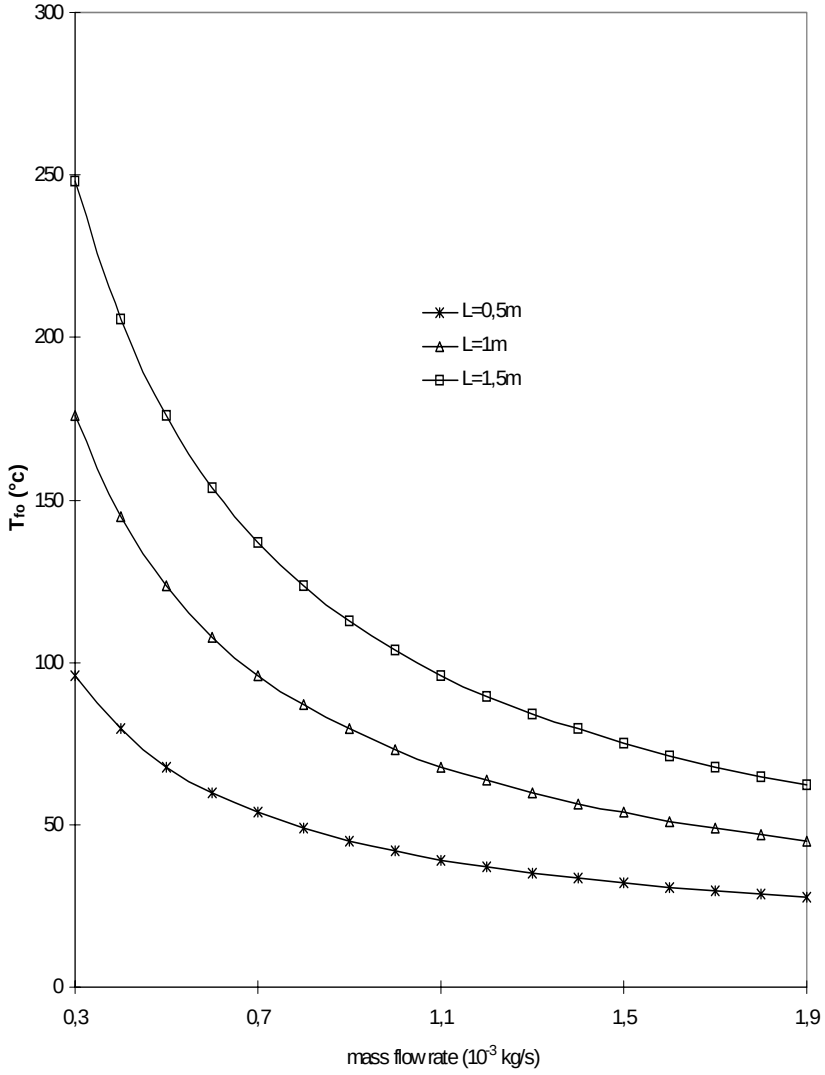

(a)

Figure 6a: The outlet temperature as function of mass flow rate at t_M=12pm30 for some values of L (a) Type 1, (b) Type 2, T_{fe}=10,0°c; V=5,0 m/s

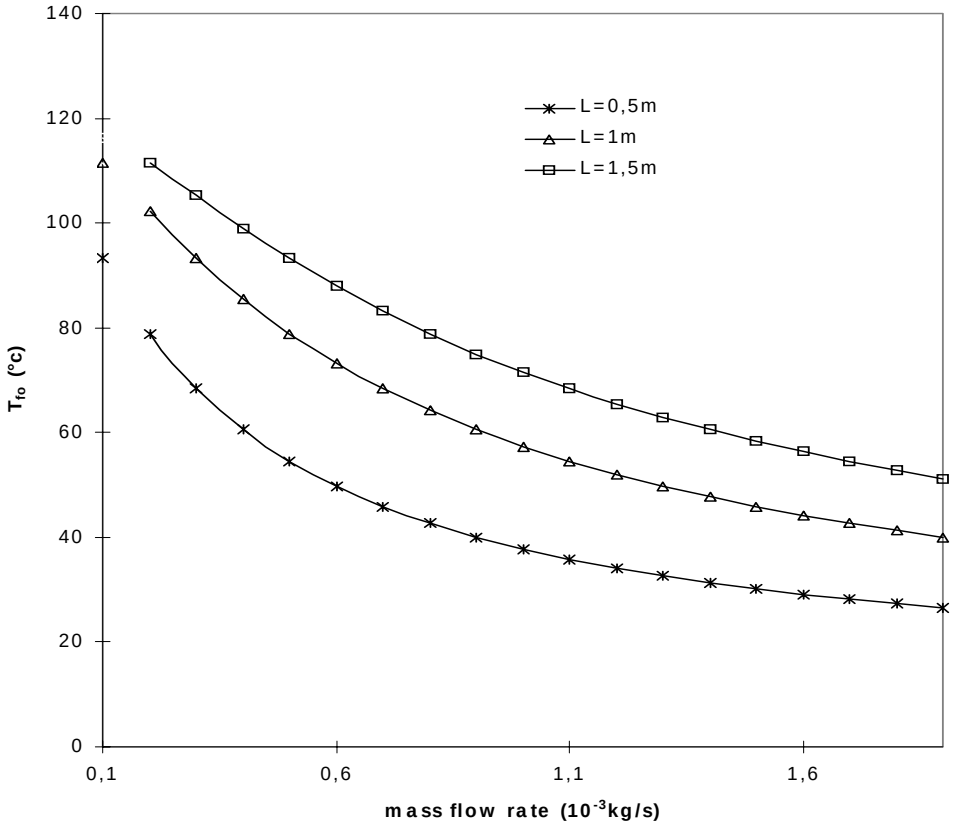

Figure 6b: The outlet temperature as function of mass flow rate at t_M=12pm30 for some values of L (a) Type 1, (b) Type 2, T_{fe}=10,0°c; V=5,0 m/s

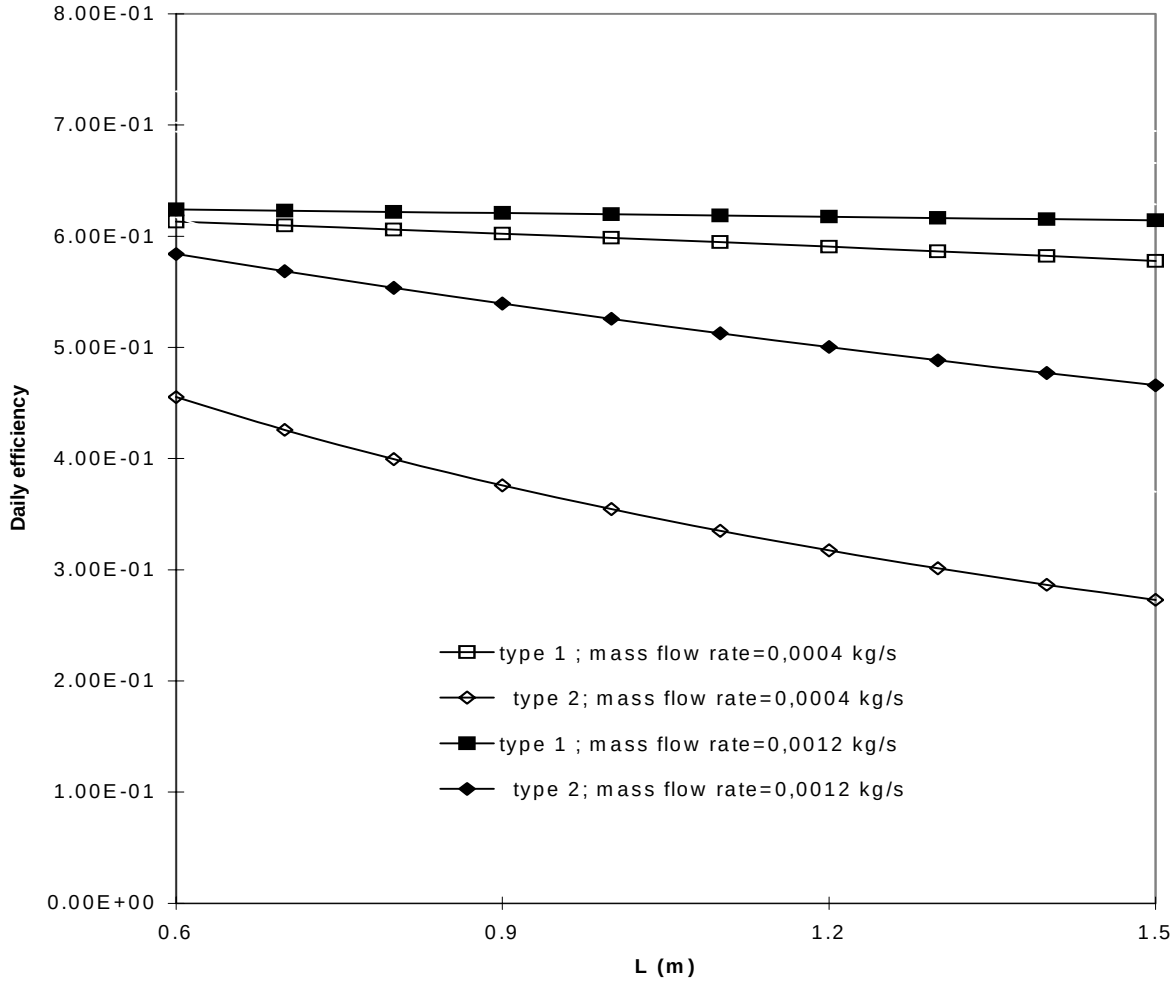

Figure 7: The efficiency as a function of plate length; T_{fe}=10,0°c; V=5,0 m/s

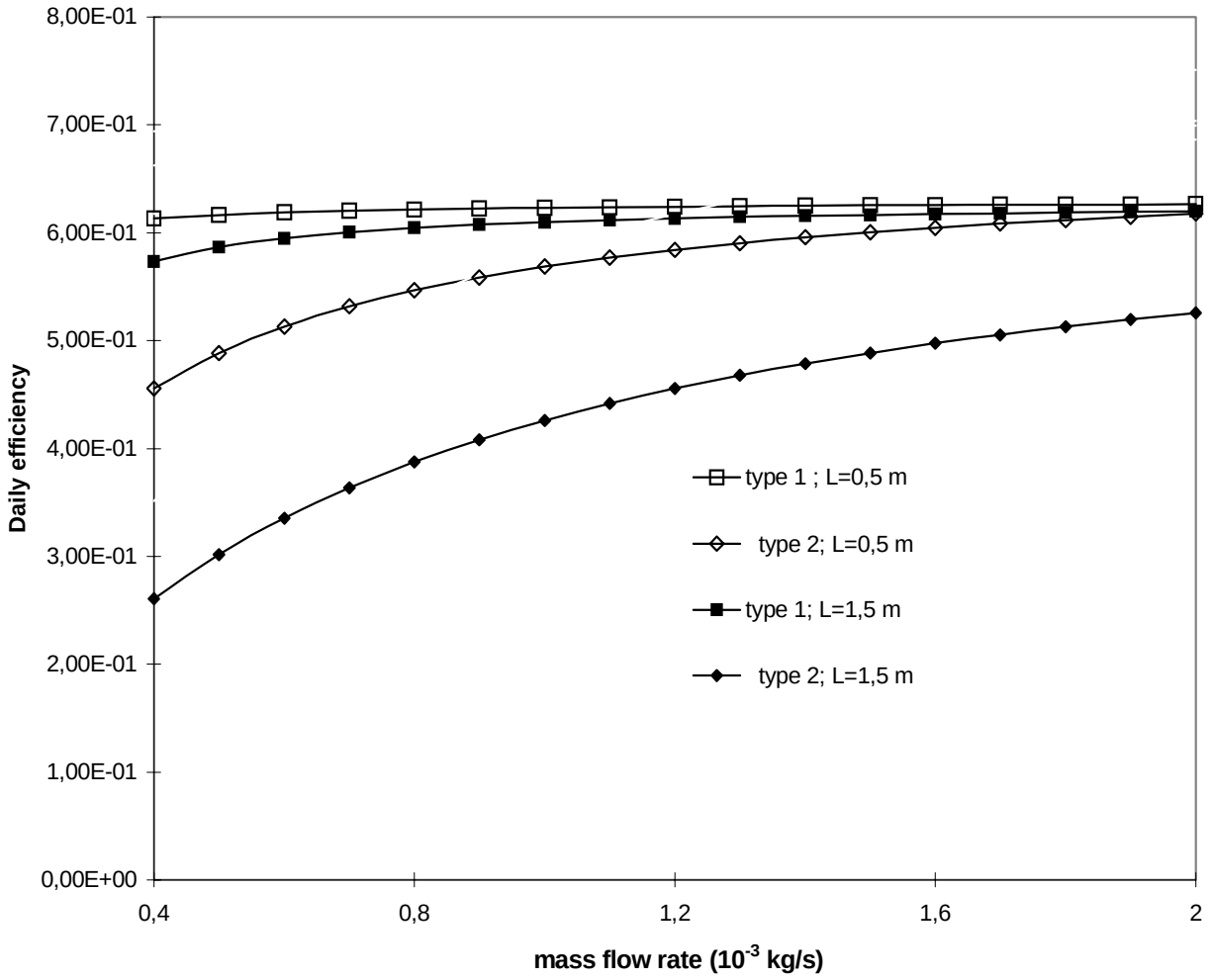

Figure 8: The efficiency as function of mass flow rate;
T_{fe}=10,0°c; V=5,0 m/s

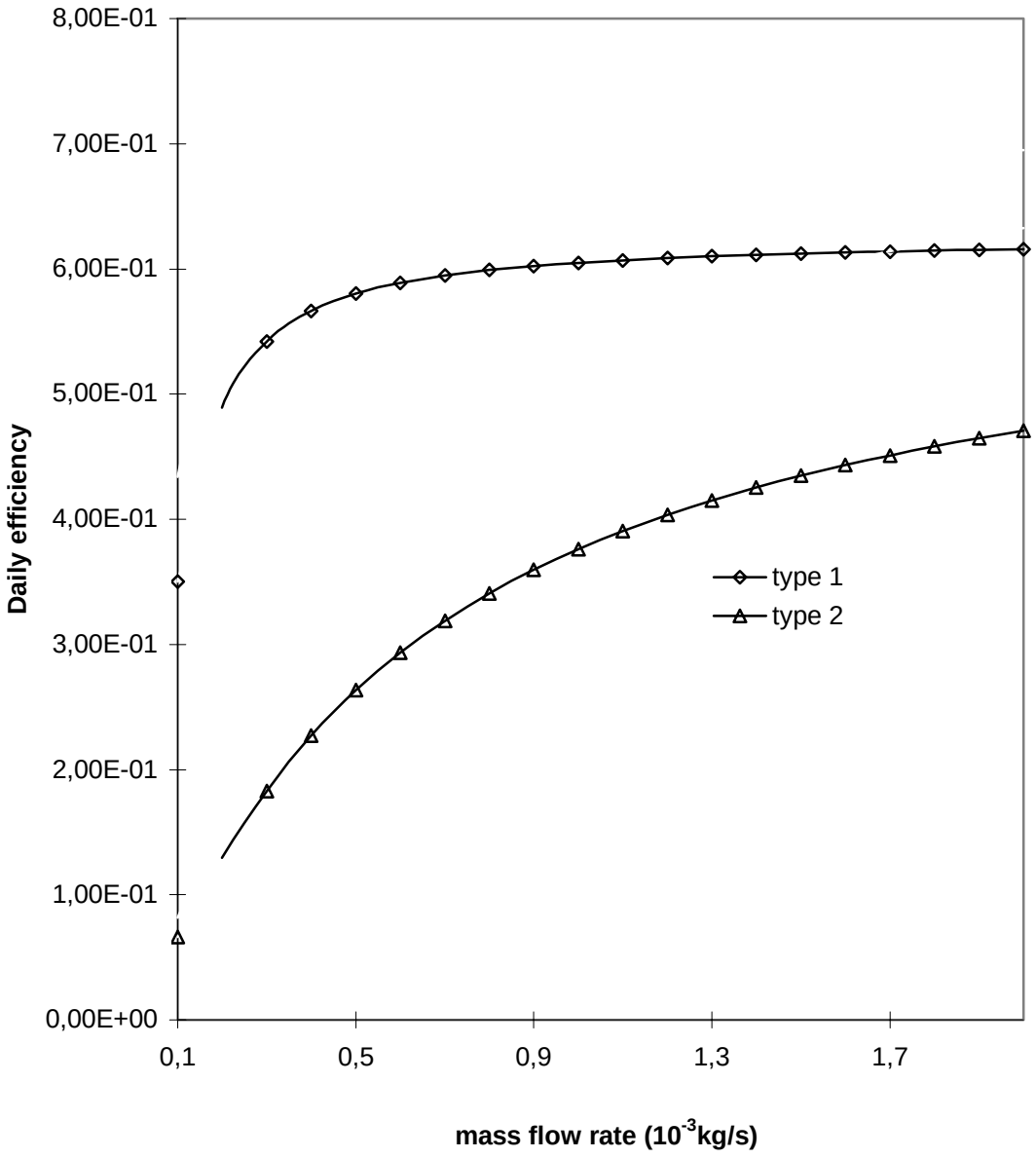

Figure 8-bis: The efficiency as function of mass flow rate for L=1,5 m T_{fe}=20,0°; V=5,0 m/s

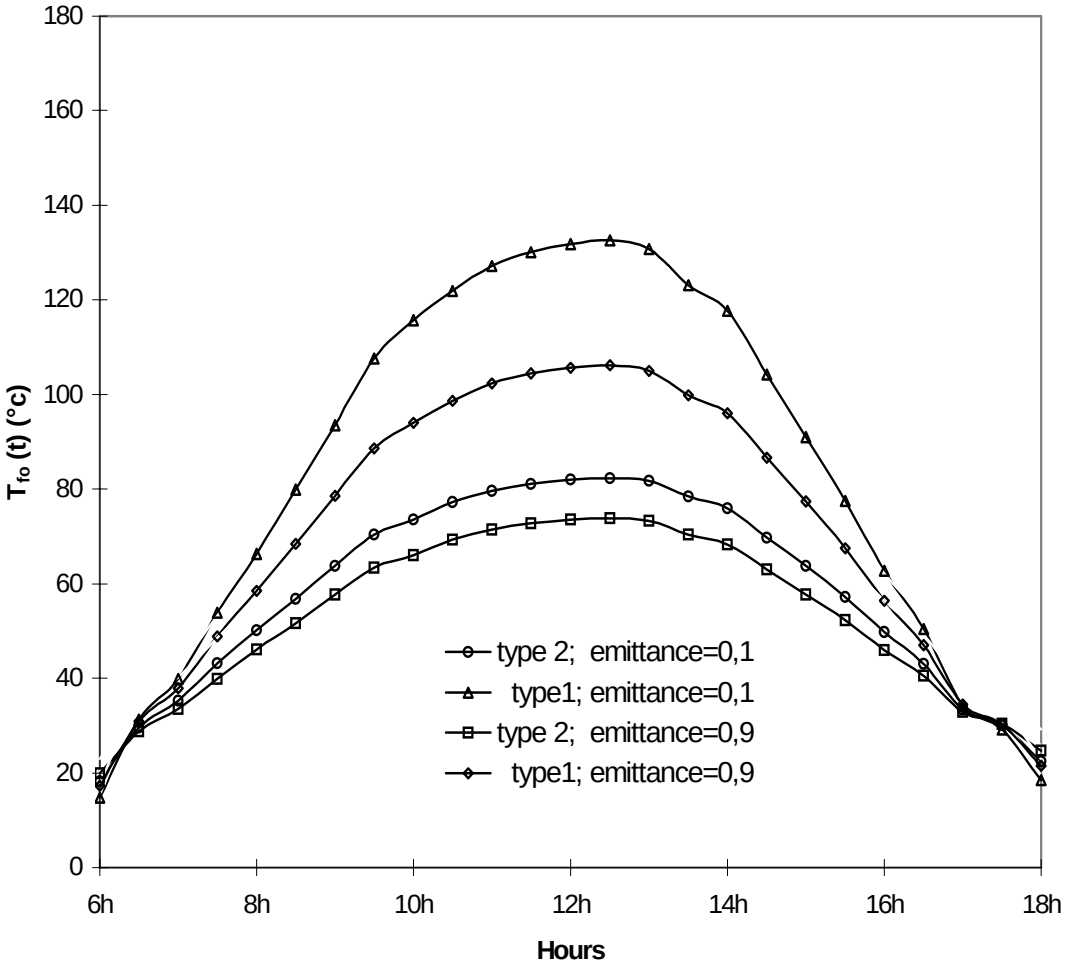

Figure 9: Outlet temperature as a function of type of surface
mass flow rate=0,0008 kg/s; T_{fe}=10,0°c; V=5,0 m/s

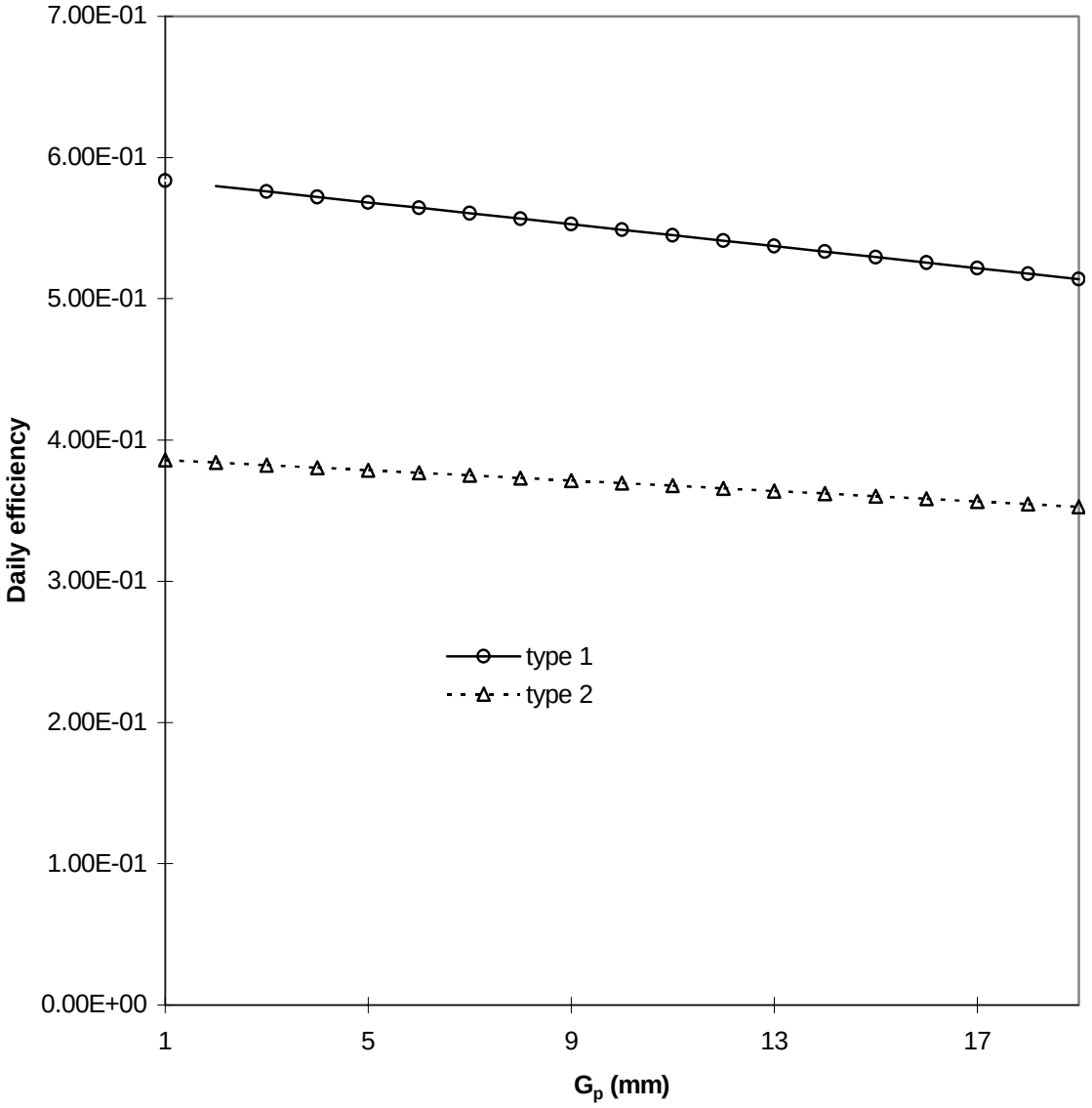

Figure 10: Effect of the gap size G_p on the daily efficiency of the Types 1 and 2, V=5,0 m/s; T_{fe}=10,0°c; mass flow rate=0,0008 kg/s

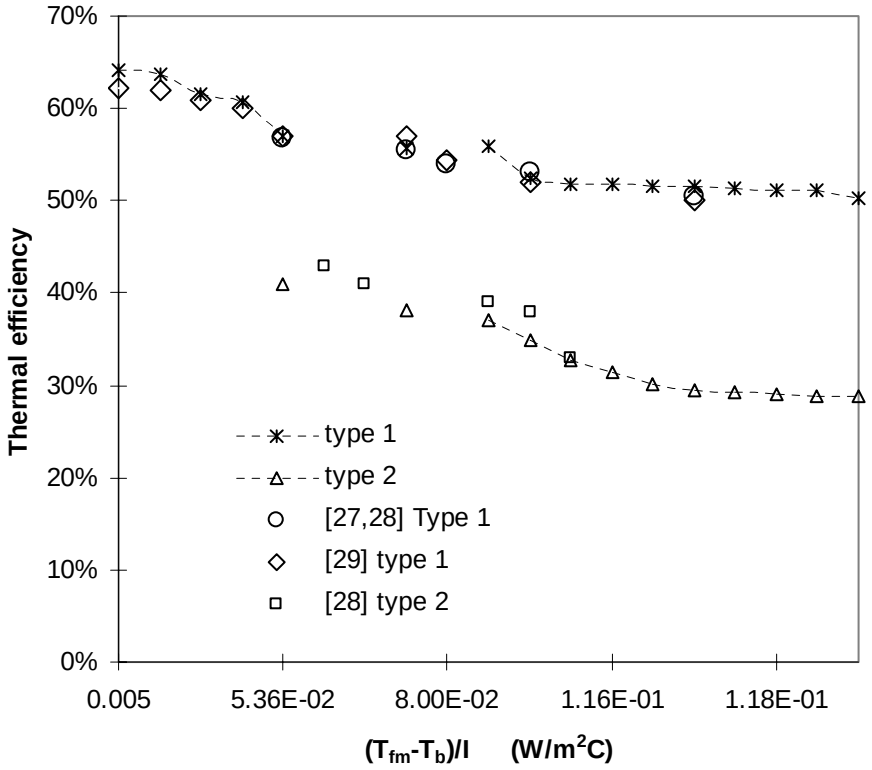

Figure 11: Comparison of Collectors efficiencies